

Synthesis, Characterization, and Stability of Dealkylated Salen-Supported Aluminum Phosphates

Rahul R. Butala,* Sean Parkin, John H. Walrod, and David A. Atwood

Cite This: <https://doi.org/10.1021/acs.inorgchem.0c03244>

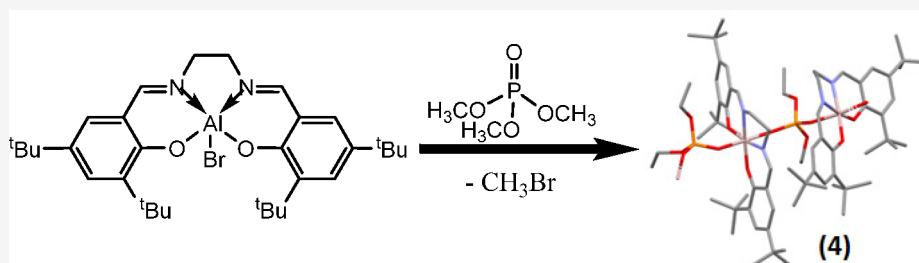
Read Online

ACCESS |

Metrics & More

Article Recommendations

Supporting Information



ABSTRACT: Three salen aluminum bromide compounds salen(^tBu)AlBr (**1**) (salen = *N,N'*-ethylenebis(3,5-di-*tert*-butylsalicylideneimine)), salpen(^tBu)AlBr (**2**) (salpen = *N,N'*-propylenebis(3,5-di-*tert*-butylsalicylideneimine)), and salophen(^tBu)AlBr (**3**) (salophen = *N,N'*-*o*-phenylenebis(3,5-di-*tert*-butylsalicylideneimine)) were evaluated for their potential use as dealkylation agents with a series of organophosphates. These reactions led to the aluminum phosphate compounds containing six-coordinate aluminum centers and hydrolytically stable P–O–C bonds: **4** = [salen(^tBu)AlOP(O)(OMe)₂]_{*n*}, **5** = [salen(^tBu)AlOP(O)(OEt)₂]_{*n*}, **6** = [salen(^tBu)AlOP(O)(OPh)₂]_{*n*}, **7** = [salophen(^tBu)AlOP(O)(OMe)₂]_{*n*}, **8** = [salpen(^tBu)AlOP(O)(O^{*i*}Pr)₂]_{*n*}, **9** = (salen(^tBu)AlO)₃PO, **10** = (salpen(^tBu)AlO)₃PO, **11** = (salophen(^tBu)AlO)₃PO. All the compounds were characterized by ¹H, ¹³C, ²⁷Al, and ³¹P NMR, IR, and mass spectrometry. Furthermore, compounds **4**–**8** were structurally characterized by single-crystal X-ray diffraction. The potential hydrolysis of these compounds was modeled with **4** and demonstrated the unique stability of the final product and ease of isolation.

1. INTRODUCTION

Organophosphates are important compounds found in nerve gas agents and pesticides. Despite a global ban on the production and use of nerve agents, these chemicals pose a threat in both active war zones and aging weapon stockpiles.^{1–3} The persistent search for efficient and reliable remediation technologies for nerve agent destruction remains an important challenge in science. Cleavage of the P–O–C bond via dealkylation in these compounds is considered an effective method of decontamination.^{4,5} However, for effective use of this chemistry, the resulting products of this reaction must be nontoxic, easy to handle, and stable to environmental conditions such as hydrolysis.

Aluminum-phosphate based materials are useful in a number of applications, including nerve gas decontamination, catalysts or catalyst supports, nonreactive fillers in polymeric composites, analytical and industrial adsorbents, and flame-retardants.^{6–8} Structures with evolving levels of complexity as one-dimensional chains, porous two-dimensional layers, and three-dimensional open-framework materials are possible.⁹ Nonaqueous synthetic routes are useful for the production of unique molecular aluminophosphates with well-defined structures compared to the traditional hydrothermal synthesis with aluminum and phosphorus precursors.^{10–13} The alumi-

num center in aluminophosphates can exhibit different coordination numbers: four,¹⁴ five,¹⁵ and six.¹⁶

Previous work has demonstrated that mononuclear Schiff base aluminum compounds, Salen-AlBr, dealkylate a series of organophosphates under mild conditions.¹⁷ The products from these reactions included various alkyl bromides and an unidentified aluminum phosphate compound that remained in solution.¹⁸ Herein, we have structurally characterized the resulting products of dealkylation of nontoxic alkyl phosphates with salen aluminum bromide compounds (SAB) as single crystals suitable for X-ray diffraction. In addition, this work explores total dealkylation with different phosphates as a function of structure and evaluates the hydrolytic stability of the reaction products with Al–O–P bonds for the potential destruction of nerve agents.

Received: November 2, 2020

2. EXPERIMENTAL SECTION

2.1. Reagents. The following reagents and solvents were obtained commercially and used as received: aluminum bromide (anhydrous, 99.9%), triethylaluminum (>93%), trimethyl phosphate ($\geq 99\%$), triethyl phosphate ($\geq 99.8\%$), triisopropyl phosphate (>99%), and 2-ethylhexyldiphenyl phosphate ($\geq 99\%$) from Sigma-Aldrich; deuterium oxide (100%) and CDCl_3 (99.9%) from Cambridge Isotope Laboratories Inc.; chloroform (99.8%) and toluene (99.8%) from Fisher Scientific; water was distilled and deionized (18 M Ω cm).

2.2. Analytical Techniques. All air-sensitive manipulations were conducted using Schlenk line techniques in conjunction with an inert-atmosphere glovebox. All solvents were rigorously dried prior to use. $\text{Salen}(\text{Bu})\text{AlBr}$, $\text{salpen}(\text{Bu})\text{AlBr}$, and $\text{salophen}(\text{Bu})\text{AlBr}$ were synthesized according to the literature procedure.¹⁸ NMR data were obtained on a Varian Inova-400 instrument. Chemical shifts are reported relative to SiMe_4 for ^1H , AlBr_3 (1.1 M in D_2O) for ^{27}Al , and 85% H_3PO_4 for ^{31}P . Infrared spectra were recorded at room temperature in a potassium bromide pellet on a Nicolet iS10 spectrometer. X-ray data were collected on a Bruker-Nonius X8 Proteum (Cu $K\alpha$ radiation) diffractometer. All calculations were performed using the SHELX software package.¹⁹ The structures were solved by direct methods,²⁰ and successive interpretation of difference Fourier maps were followed by least-squares refinement.²¹ All non-hydrogen atoms were refined anisotropically. The hydrogen atoms were included using a riding model with isotropic parameters tied to the parent atom. Crystallographic data were deposited with the Cambridge Crystallographic Data Center (CCDC) reference nos: 1996252, 1996253, 1996254, 1996255, and 1996256.

2.3. Synthesis of $[\text{Salen}(\text{Bu})\text{AlOP}(\text{O})(\text{OMe})_2]_n$ (4). To a rapidly stirred solution of $\text{salen}(\text{Bu})\text{AlBr}$ (3.0 g, 5.02 mmol) in chloroform (15 mL) was added trimethyl phosphate (0.7 g, 5.02 mmol). The reaction mixture was stirred for 24 h at room temperature and filtered. The volatiles were removed under vacuum from the pale yellow filtrate to give a yellow solid, which was purified by recrystallization from toluene. Single crystals suitable for X-ray analysis were grown by slow evaporation of a 1:1 toluene/dichloromethane mixture. Yield: 2.6 g (80%). Mp.: 310–312 °C. ^1H NMR (CDCl_3 , 400 MHz): 1.27 (s, 18H, $\text{C}(\text{CH}_3)_3$), 1.46 (s, 18H, $\text{C}(\text{CH}_3)_3$), 3.08 (d, 6H, phosphate OCH_3), 3.79 (s, br, 2H, NCH_2), 4.37 (s, br, 2H, NCH_2), 7.04 (d, 2H, Ph-H), 7.53 (d, 2H, Ph-H), 8.38 (s, 2H, $\text{N}=\text{CH}$). ^{31}P [^1H] NMR (CDCl_3 , 400 MHz): δ -6.58. IR (KBr, cm^{-1}): 3041s, 2953w, 2906w, 2867m, 1651w, 1636w, 1550m, 1537m, 1476s, 1464m, 1257w, 1219m, 1075m, 1038w, 974s, 839m, 788m, 752s, 608m, 583m. MS (EI, positive): 642 (M^+ , 24%), 585 ($\text{M}^+ - \text{Bu}$, 100%), 529 ($\text{M}^+ - 2 \text{Bu}$, 17%), 517 ($\text{M}^+ - \text{OP}(\text{O})(\text{OMe})_2$, 7%).

2.4. Synthesis of $[\text{Salen}(\text{Bu})\text{AlOP}(\text{O})(\text{OEt})_2]_n$ (5). To a rapidly stirred solution of $\text{salen}(\text{Bu})\text{AlBr}$ (0.9 g, 1.50 mmol) in chloroform (4.5 mL) was added triethyl phosphate (0.27 g, 1.505 mmol). The reaction mixture was stirred for 24 h at room temperature and filtered. The volatiles were removed under vacuum from the pale yellow filtrate to give a yellow solid, which was purified by recrystallization from toluene. Single crystals suitable for X-ray analysis were grown by slow evaporation of a dichloromethane solution. Yield: 0.80 g (80%). Mp.: 321 °C. ^1H NMR (CDCl_3 , 400 MHz): δ 0.84 (t, 6H, phosphate OCH_2CH_3), 1.29 (s, 18H, $\text{C}(\text{CH}_3)_3$), 1.52 (s, 18H, $\text{C}(\text{CH}_3)_3$), 3.58 (m, 4H, phosphate OCH_2CH_3), 3.74 (s, br, 2H, NCH_2), 4.34 (s, br, 2H, NCH_2), 7.05 (d, 2H, Ph-H), 7.54 (d, 2H, Ph-H), 8.41 (s, 2H, $\text{N}=\text{CH}$). ^{31}P [^1H] NMR (CDCl_3 , 400 MHz): δ -8.00. IR (KBr, cm^{-1}): 3042s, 2956w, 2905w, 2868m, 1648w, 1545w, 1537m, 1477s, 1443m, 1245w, 1169m, 1060m, 965s, 874m, 787m, 753s, 606m, 583m. MS (EI, positive): 670 (M^+ , 24%), 613 ($\text{M}^+ - \text{Bu}$, 100%), 517 ($\text{M}^+ - \text{OP}(\text{O})(\text{OEt})_2$, 7%).

2.5. Synthesis of $[\text{Salen}(\text{Bu})\text{AlOP}(\text{O})(\text{OPh})_2]_n$ (6). To a rapidly stirred solution of $\text{salen}(\text{Bu})\text{AlBr}$ (1.05 g, 1.75 mmol) in chloroform (5 mL) was added 2-ethylhexyldiphenyl phosphate (0.636 g, 1.75 mmol). The reaction mixture was stirred for 24 h at room temperature and filtered. The volatiles were removed under vacuum from the pale yellow filtrate to give a yellow solid. Yield: 0.82 g (61%). Mp.: 262 °C. ^1H NMR (CDCl_3 , 400 MHz): δ 1.32 (s, 18H,

$\text{C}(\text{CH}_3)_3$), 1.48 (s, 18H, $\text{C}(\text{CH}_3)_3$), 3.68 (s, br, 2H, NCH_2), 4.25 (s, br, 2H, NCH_2), 6.75–7.02 (m, 10H, P-O- C_6H_5), 7.01 (d, 2H, Ph-H), 7.55 (d, 2H, Ph-H), 8.32 (s, br, 2H, $\text{N}=\text{CH}$). ^{31}P [^1H] NMR (CDCl_3 , 400 MHz): δ -19.88. IR (KBr, cm^{-1}): 3064s, 3043s, 2954w, 2903m, 2867m, 1643w, 1594w, 1538w, 1492m, 1477s, 1442m, 1235w, 1207m, 1122m, 941s, 814m, 753m, 607m. MS (EI, positive): 760 (M^+ , 30%), 709 ($\text{M}^+ - \text{Bu}$, 100%), 633 ($\text{M}^+ - \text{Bu} - \text{Ph}$, 15%), 517 ($\text{M}^+ - \text{OP}(\text{O})(\text{OPh})_2$, 18%).

2.6. Synthesis of $[\text{Salophen}(\text{Bu})\text{AlOP}(\text{O})(\text{OMe})_2]_n$ (7). To a rapidly stirred solution of $\text{salophen}(\text{Bu})\text{AlBr}$ (0.84 g, 1.30 mmol) in chloroform (4 mL) was added trimethyl phosphate (0.18 g, 1.30 mmol). The reaction mixture was stirred for 24 h at room temperature and filtered. The volatiles were removed under vacuum from the pale yellow filtrate to give a yellow solid, which was purified by recrystallization from a 1:1 toluene/hexane mixture. Single crystals suitable for X-ray analysis were grown by slow evaporation of a chloroform solution. Yield: 0.68 g (76%). Mp.: 344 °C. ^1H NMR (CDCl_3 , 400 MHz): δ 1.36 (s, 18H, $\text{C}(\text{CH}_3)_3$), 1.53 (s, 18H, $\text{C}(\text{CH}_3)_3$), 3.04 (d, 6H, phosphate OCH_3), 7.191 (d, 2H, Ph-H), 7.37 (m, 4H, Ph-H), 7.61 (d, 2H, Ph-H), 8.81 (s, br, 2H, $\text{N}=\text{CH}$). ^{31}P [^1H] NMR (CDCl_3 , 400 MHz): δ -6.94. IR (KBr, cm^{-1}): 2950w, 2904m, 2866m, 2359s, 1617w, 1584w, 1531m, 1475s, 388m, 1218w, 1196m, 1051m, 863s, 846m, 594m, 564s. MS (EI, positive): 690 (M^+ , 63%), 675 ($\text{M}^+ - \text{CH}_3$, 96%), 550 ($\text{M}^+ - \text{CH}_3 - \text{OP}(\text{O})(\text{OCH}_3)_2$, 100%).

2.7. Synthesis of $[\text{Salpen}(\text{Bu})\text{AlOP}(\text{O})(\text{O}^i\text{Pr})_2]_2$ (8). To a rapidly stirred solution of $\text{salpen}(\text{Bu})\text{AlBr}$ (1.43 g, 2.33 mmol) in chloroform (7 mL) was added triisopropyl phosphate (0.52 g, 2.33 mmol). The reaction mixture was stirred for 24 h at room temperature and filtered. The volatiles were removed under vacuum from the pale yellow filtrate to give a yellow solid, which was purified by recrystallization from toluene. Yield: 1.0 g (60%). Mp.: 248 °C. ^1H NMR (CDCl_3 , 400 MHz): δ 0.91 (d, 12H, phosphate $\text{OCH}(\text{CH}_3)_2$), 1.29 (s, 18H, $\text{C}(\text{CH}_3)_3$), 1.48 (s, 18H, $\text{C}(\text{CH}_3)_3$), 2.21 (m, 1H, $\text{OCH}_2\text{CH}_2\text{CH}_2$), 2.29 (m, 1H, $\text{CH}_2\text{CH}_2\text{CH}_2$), 3.68 (m, 2H, phosphate $\text{OCH}(\text{CH}_3)_2$), 4.19 (m, 4H, NCH_2), 7.02 (d, 2H, Ph-H), 7.50 (d, 2H, Ph-H), 8.27 (s, 2H, $\text{N}=\text{CH}$). ^{31}P [^1H] NMR (CDCl_3 , 400 MHz): δ -11.16. IR (KBr, cm^{-1}): 3064s, 3031s, 2958w, 2898m, 2869m, 1640w, 1626w, 1551m, 1467s, 1441m, 1325w, 1263w, 1171m, 1013m, 994s, 840m, 540s. MS (EI, positive): 712 (M^+ , 7%), 530 ($\text{M}^+ - \text{OP}(\text{O})(\text{O}^i\text{Pr})_2$, 100%).

2.8. Synthesis of $(\text{Salen}(\text{Bu})\text{AlO})_3\text{PO}$ (9). To a rapidly stirred solution of $\text{salen}(\text{Bu})\text{AlBr}$ (0.42 g, 0.70 mmol) in chloroform (3 mL) was added trimethyl phosphate (0.033 g, 0.23 mmol). The reaction mixture was stirred for 24 h at room temperature and filtered. The volatiles were removed under vacuum from the pale yellow filtrate to give a yellow solid, which was purified by recrystallization from a 1:1 toluene/hexane mixture. Yield: 0.3 g (77%). ^1H NMR (CDCl_3 , 400 MHz): δ 1.30 (s, 18H, $\text{C}(\text{CH}_3)_3$), 1.48 (s, 18H, $\text{C}(\text{CH}_3)_3$), 3.80 (s, br, 4H, NCH_2), 7.05 (d, 2H, Ph-H), 7.52 (d, 2H, Ph-H), 8.3 (s, 2H, $\text{N}=\text{CH}$). IR (KBr, cm^{-1}): 2962m, 2905m, 2866m, 1648s, 1628s, 1544m, 1475m, 1444m, 1421w, 1390w, 1361w, 1310w, 1257w, 1180w, 867w. MS (MALDI, positive): 1648 (M^+ , 100%), 1632 ($\text{M}^+ - \text{CH}_3$, 90%).

2.9. Synthesis of $(\text{Salpen}(\text{Bu})\text{AlO})_3\text{PO}$ (10). To a rapidly stirred solution of $\text{salpen}(\text{Bu})\text{AlBr}$ (0.95 g, 1.55 mmol) in chloroform (5 mL) was added trimethyl phosphate (0.072 g, 0.52 mmol). The reaction mixture was stirred for 24 h at room temperature and filtered. The volatiles were removed under vacuum from the pale yellow filtrate to give a yellow solid, which was purified by recrystallization from a 1:1 toluene/hexane mixture. Yield: 0.6 g (69%). ^1H NMR (CDCl_3 , 400 MHz): δ 1.30 (s, 18H, $\text{C}(\text{CH}_3)_3$), 1.50 (s, 18H, $\text{C}(\text{CH}_3)_3$), 2.23 (m, 2H, $\text{CH}_2\text{CH}_2\text{CH}_2$), 3.65 (s, br, 2H, NCH_2), 4.02 (s, br, 2H, NCH_2), 7.02 (d, 2H, Ph-H), 7.50 (d, 2H, Ph-H), 8.23 (s, 2H, $\text{N}=\text{CH}$). IR (KBr, cm^{-1}): 3064s, 3031s, 2956w, 2908m, 2866m, 1640w, 1626w, 1551m, 1467s, 1441m, 1325w, 1263w, 1171m, 1013m, 994s, 840m, 540s. MS (MALDI, positive): 1750 ($\text{M}^+ + \text{CH}_3$, 100%), 1188 ($\text{M}^+ - \text{salen}$, 10%), 531 (SalenAl , 15%).

2.10. Synthesis of $(\text{Salophen}(\text{Bu})\text{AlO})_3\text{PO}$ (11). To a rapidly stirred solution of $\text{salophen}(\text{Bu})\text{AlBr}$ (0.77 g, 1.2 mmol) in

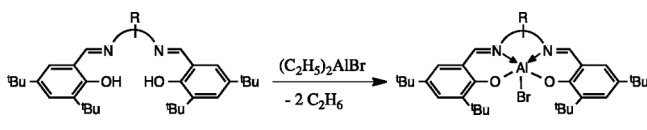
chloroform (4 mL) was added trimethyl phosphate (0.056 g, 0.40 mmol). The reaction mixture was stirred for 24 h at room temperature and filtered. The volatiles were removed under vacuum from a the pale yellow filtrate to give a yellow solid, which was purified by recrystallization from 1:1 toluene/hexane mixture. Yield: 0.5 g (70%). ^1H NMR (CDCl_3 , 400 MHz): δ 1.25 (s, 18H, $\text{C}(\text{CH}_3)_3$), 1.42 (s, 18H, $\text{C}(\text{CH}_3)_3$), 6.80 (m, 2H, Ph-H), 7.20 (d, 2H, Ph-H), 7.40 (m, 2H, Ph-H), 7.55 (d, 2H, Ph-H), 8.4 (s, 2H, N=CH). IR (KBr, cm^{-1}): 3064s, 3031s, 2961w, 2905m, 2869m, 1635w, 1626w, 1445, 1441m, 1325w, 1263w, 1171m, 1013m, 994s, 865w, 847m, 785s, 757w, 610m. MS (MALDI, positive): 1807 ($\text{M}^+ + \text{CH}_3$, 20%), 1256 ($\text{M}^+ - \text{salen}$, 100%).

2.11. Aqueous Stability Study. Nitrogen was bubbled through deionized water at atmospheric pressure and 25 °C for a specified period of time. The initial pH was 6.7. $\text{Salen}(\text{tBu})\text{AlOP}(\text{O})(\text{OMe})_2$ (2.0 g, 3.1 mmol) was added to 20 mL of water and stirred for 3 weeks under a N_2 atmosphere. The yellow slurry was filtered and washed with water. Recovery: 1.9 g (95%). Mp.: 309–312 °C. ^1H NMR (CDCl_3 , 400 MHz): 1.27 (s, 18H, $\text{C}(\text{CH}_3)_3$), 1.46 (s, 18H, $\text{C}(\text{CH}_3)_3$), 3.08 (d, 6H, phosphate OCH_3), 3.9 (s, br, 4H, NCH_2), 7.04 (d, 2H, Ph-H), 7.53 (d, 2H, Ph-H), 8.38 (s, 2H, N=CH). IR (KBr, cm^{-1}): 3447w, 3041s, 2953w, 2906w, 2867m, 1651w, 1636w, 1550m, 1537m, 1476s, 1464m, 1257w, 1219m, 1075m, 1038w, 974s, 839m, 788m, 752s, 608m, 583m. MS (EI, positive): 642 (M^+ , 24%), 585 ($\text{M}^+ - \text{tBu}$, 100%), 529 ($\text{M}^+ - 2 \text{tBu}$, 17%), 517 ($\text{M}^+ - \text{OP}(\text{O})(\text{OMe})_2$, 7%).

3. RESULTS AND DISCUSSION

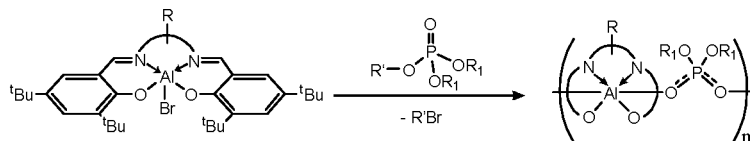
3.1. Synthesis and Characterization. SAB compounds 1–3 were prepared by combining diethylaluminum bromide and the corresponding $\text{salen}(\text{tBu})\text{H}_2$ ligands according to literature procedures, as shown in Scheme 1.¹⁸ Dealkylation of

Scheme 1. General Synthesis of $\text{Salen}(\text{tBu})\text{AlBr}$ [$\text{R} = (\text{CH}_2)_2$; Salen (1), $\text{R} = (\text{CH}_2)_3$; Salpen (2), $\text{R} = o\text{-C}_6\text{H}_4$; Salophen (3)]



different alkyl phosphates was carried out using compounds 1–3 in an equimolar ratio to give stable six-coordinate salen aluminum phosphates, 4–8, and alkyl bromide derivatives, as shown in Scheme 2. The compounds were isolated by removing solvent under vacuum and purified by recrystalliza-

Scheme 2. General Synthesis of Compounds 4–8^a



R	R ₁	R'	Name	%Yield
(CH ₂) ₂	CH ₃	CH ₃	[salen(tBu)AlOP(O)(OCH ₃) ₂] _n (4)	80
(CH ₂) ₂	CH ₃ CH ₂	CH ₃ CH ₂	[salen(tBu)AlOP(O)(OCH ₂ CH ₃) ₂] _n (5)	80
(CH ₂) ₂	C ₆ H ₅	CH ₃ (CH ₂) ₃ (CH ₂ CH ₃)CHCH ₂	[salen(tBu)AlOP(O)(OPh) ₂] _n (6)	61
<i>o</i> -C ₆ H ₄	CH ₃	CH ₃	[salophen(tBu)AlOP(O)(OCH ₃) ₂] _n (7)	76
(CH ₂) ₃	CH(CH ₃) ₂	CH(CH ₃) ₂	[salpen(tBu)Al(O)P(O)(O ⁱ Pr) ₂] (8)	60

^aCompounds 4–7 are oligomers, whereas 8 is a dimer.

tion from hot toluene. SAB compounds readily form cations by the replacement of bromide by Lewis bases.¹⁸ Thus, it is likely that SAB cation formation and displacement of the bromide anion is concomitant with coordination via phosphoryl oxygen to aluminum. This coordination increases electron deficiency and activates the α carbon of the phosphate for nucleophilic attack by bromide.

The percent conversion was comparable to that of the binuclear salen boron bromide (SBB) compounds $\text{salen}(\text{tBu})\text{[BBr}_2\text{]}_2$.²² In comparison, the yield was much higher than the transformation with $\text{salen}(\text{tBu})\text{AlCl}$, 55%.¹⁸ The difference between halogens is likely attributable to lower bond strengths for Al–Br (430 kJ mol^{-1}) compared to Al–Cl (511 kJ mol^{-1}) and ease of cation formation. Shortening of the carbon chain ligand backbone resulted in higher dealkylation activity where $\text{salen}(\text{tBu})\text{AlBr}$ (1) > $\text{salpen}(\text{tBu})\text{AlBr}$ (2) > $\text{salopen}(\text{tBu})\text{AlBr}$ (3). This result was postulated as an influence of inductive effects and hyperconjugation on the electropositive character of the aluminum atom.²³ The percentage dealkylation was greater for short and straight chain phosphates compared to those with long and branched chains. For example, with $\text{salen}(\text{tBu})\text{AlBr}$ (1), the percentage conversion was 80% for trimethyl and triethyl phosphate compared to 61% for 2-ethylhexyldiphenyl phosphate.

Compounds 4–8 were characterized by NMR, IR, and MS. For the ^{27}Al NMR spectra, no peak was detected for compounds 4–7. This is probably due to asymmetrical substitution of aluminum nuclei, resulting in a very short relaxation time. The ^{27}Al NMR for 8 shows two broad peaks. The peak at δ 0.1 ppm represents six-coordinate aluminum, and the peak at δ 30 ppm corresponds to five-coordinate aluminum.²⁴ Thus, the solution product for 8 appears to be different from the solid-state structure found in the X-ray crystal studies where the aluminum atom is six-coordinate. In solution (CDCl_3), it is possible one of the two bound phosphate linkages dissociates, making the aluminum five-coordinate. This hypothesis was supported using variable-temperature ^{27}Al NMR. As the temperature of the sample was lowered, the peak intensity at δ 30 ppm decreased and eventually disappeared at -50 °C. The ^1H NMR spectra of 4–8 were very close to that of the salen aluminum phosphinate analogue reported previously.²⁵

The ^1H spectra of 4–8 show two singlets for tBu groups of the ligand in the range of δ 1.29–1.50 ppm, each peak

corresponding to 18 protons. However, only one imine singlet in the range of δ 8.3–8.8 indicates symmetric geometry around the ligand backbone for these compounds in solution. There are multiple CH_2 peaks corresponding to the alkylene backbone protons from the ligand. For 4–6, two methylene peaks corresponding to the backbone protons appear at δ 3.7 and 4.20 ppm, respectively. The ^1H NMR spectrum of compound 8 contains a multiplet at δ 2.11, 2.29, and 4.19 corresponding to protons from the ligand backbone ($\text{CH}_2\text{CH}_2\text{CH}_2$). Protons from only two alkyl groups of phosphates were observed in the ^1H spectra of 4–8. Thus, this indicated cleavage of one of the three P–O–C linkages. The ^{31}P NMR spectra of 4–8 contain single peaks at δ –6.58, –8.00, –19.87, –6.94, and –11.16, respectively. These ^{31}P NMR shifts are upfield from the chemical shifts of the starting trialkylphosphate (Table 1) and are consistent with Al–O–P bonding with coordination of the phosphoryl oxygen to the electropositive aluminum atom.

Table 1. ^{31}P NMR Shifts for Compounds 4–8

compound	δ ^{31}P	starting alkyl phosphate	δ ^{31}P
4	–6.58	trimethyl phosphate	3.01
5	–8.00	triethyl phosphate	–0.24
6	–19.88	2-ethylhexyldiphenyl phosphate	–11.09
7	–6.94	trimethyl phosphate	3.01
8	–11.16	triisopropyl phosphate	–3.43

3.2. Total Dealkylation. Total dealkylation of trimethyl phosphate was carried out using compounds 1–3 in stoichiometric amounts (3 equiv of SAB to 1 equiv of phosphate) to give fully dealkylated products 9–11 via cleavage of all three C–O bonds. As seen in Scheme 3, the trend in percent conversion for total dealkylation was similar to the results in Scheme 2. Shortening of the ligand backbone carbon atoms resulted in slightly higher dealkylation activity. However, the influence of inductive effects and resulting electropositive character of aluminum were not as dominant. Although attempts to isolate single crystals suitable for X-ray crystallography were not successful, ^1H , IR, and MS (MALDI) analyses support the formation of fully dealkylated phosphate.

It was observed that the ^1H NMR spectra have peaks corresponding to the ligand only, and no peak corresponding to the methoxy group of phosphate. The MALDI mass spectra of 9, 10, and 11 show molecular ion peaks at m/z 1648, 1705, and 1807, respectively. The isotope patterns from these spectra were very similar to the isotope pattern obtained from the

simulation experiment. For example, mass spectra of compound 9 (Figure S1A) contained six isotope peaks at m/z 1648 (93%), 1649 (100%), 1650 (55%), 1651 (22%), 1652 (7%), and 1653 (2%), which is in good agreement with isotope simulation for the molecular formula of compound 9 ($\text{C}_{96}\text{H}_{139}\text{O}_{10}\text{N}_6\text{Al}_3\text{P}$) (Figure S1B).

3.3. Solid-State Structures. The solid-state structures of compounds 4–8 were determined by single-crystal X-ray diffraction. Single crystals suitable for X-ray crystallography were obtained by slow evaporation of either dichloromethane or chloroform. The molecular structure of 7 reveals the formation of polymeric chains of salenAl connected by O–P–O bonds (Figure 1). A similar polymer formation was observed

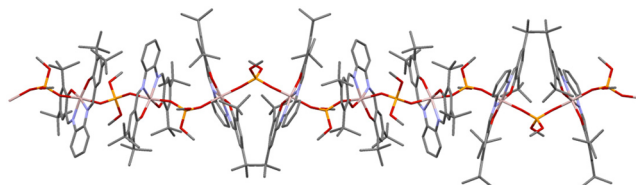


Figure 1. Polymeric chain formed by Al–O–P linkages in compound 7.

for compounds 4, 5, and 6. Table S2 lists selected bond lengths and angles, while the data collection parameters are listed in Table S1.

Compounds 5 and 6 crystallized with orthorhombic space groups $P2_12_12_1$ and $Fddd$, respectively. In comparison, compounds 4 and 7 crystallized with tetragonal space groups $P4_1$ and $P4_12_2$, respectively. Each of these structures contained a six-coordinate aluminum atom with distorted octahedral geometry (Figures 2, 3, 4, and 5). The axial Al–O bond

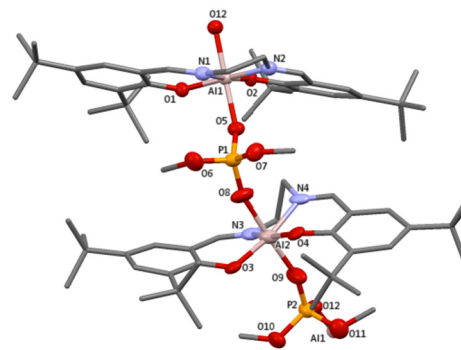
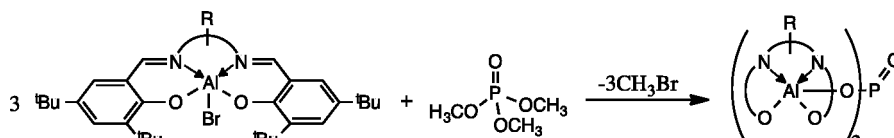


Figure 2. Crystal structure of 4.

Scheme 3. General Synthesis of Compounds 9–11



R	Name	% Yield
(CH_2) ₂	(salen(^t Bu)AlO) ₃ PO (9)	76.9%
(CH_2) ₃	(salpen(^t Bu)AlO) ₃ PO (10)	69.0
<i>o</i> -C ₆ H ₄	(salophen(^t Bu)AlO) ₃ PO (11)	70.4%

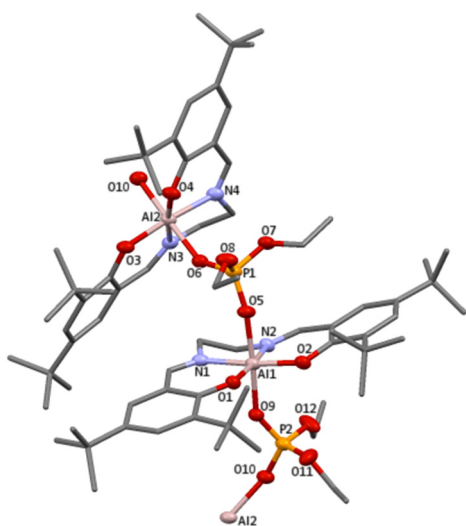


Figure 3. Crystal structure of 5.

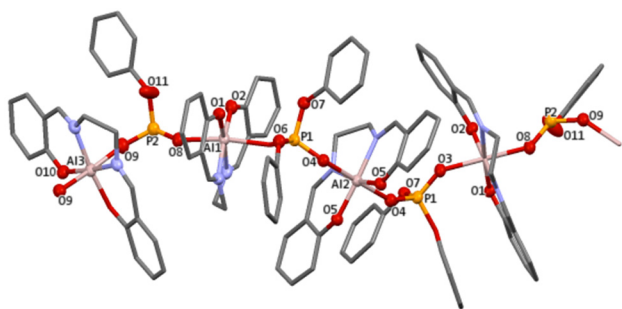


Figure 4. Crystal structure of 6.

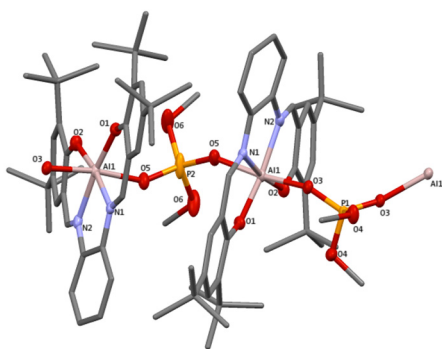


Figure 5. Crystal structure of 7.

distances (~ 1.90 – 1.92 Å) are longer than equatorial Al–O bond distances (~ 1.80 – 1.82 Å) due to the greater steric requirements of the axial groups. The axial O–Al–O bond angles are distorted (~ 171.7 – 174.5°) from ideal linearity. All P atoms have distorted tetrahedral geometry with bond angles ranging from about 100.4° to 119° . These angles compare similarly to the polymeric six-coordinate aluminum phosphinate, $[\text{salen}(\text{tBu})\text{Al}(\text{O}_2\text{P}(\text{H})\text{Ph})]_n$.²⁶ In comparison, less distortion was observed in derivatives containing four-coordinate aluminum such as $[(\text{tBu})_2\text{AlO}_2\text{P}(\text{OC}_6\text{H}_5)_2]_2$ ¹⁶ and $[\text{Me}_2\text{AlO}_2\text{POSiMe}_3]_2$.²⁷ Interestingly, out of the four P–O bonds around the phosphorus center, the bridging O–P–O bond lengths (~ 1.48 – 1.49 Å) are shorter than the other two nonbridging P–O bonds lengths, which were longer (~ 1.56 – 1.58 Å) with more single bond (1.56 Å) character

(Table S2). All Al–O–P bonds were bent in all four compounds. For compounds 4–6, there was a noticeable difference in the degree of the Al–O–P bond bending; one of the two Al–O–P bonds around the phosphorus atom was less bent than the other. For example, in compound 4, the Al1–O5–P1 ($145.69(16)^\circ$) angle was less bent than the Al2–O8–P1 ($161.10(4)^\circ$) angle. However, in compound 7, both Al–P–O bond angles are similar ($150.06(11)^\circ$ and $148.87(10)^\circ$).

The dimeric compound $[\text{salpen}(\text{tBu})\text{AlOP}(\text{O})(\text{O}^i\text{Pr})_2]_2$ (8) resulted from the dealkylation reaction of $\text{salpen}(\text{tBu})\text{AlBr}$ with triisopropyl phosphate in chloroform at room temperature. Selected bond lengths and angles are listed in Table S2, and the crystal data collection parameters are shown in Table S1. Compound 8 crystallized with the monoclinic space group $P2_1/c$. The cyclic aluminum-phosphate molecular structure of 8 formed by the combination of two salen aluminum units and two mono-dealkylated phosphate units (Figure 6). Interest-

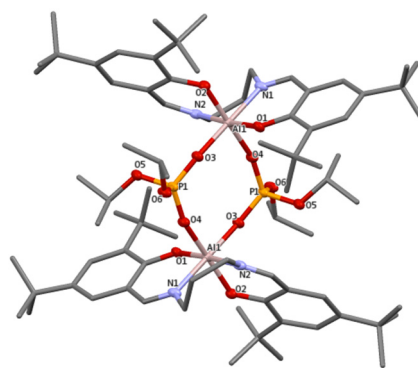


Figure 6. Crystal structure of 8.

ingly, increased flexibility of the ligand backbone resulted in dimerization rather than polymerization. The cyclic P–O bond distances for P1–O3 and P1–O4 (1.4856 and 1.4886 Å) were similar and in the range of the P–O double bond (Table S2). The other P–O distances of P1–O5 and P1–O6 (1.5735 and 1.5805 Å) are longer and in the range of P–O single bonds.

Each phosphorus atom in 8 contained distorted tetrahedral geometry. Here, angle distortion was most pronounced for the O–P–O bonds (118.81°) inside the linking cyclic aluminophosphate structure. Each aluminum atom was six-coordinate with distorted octahedral geometry. The axial and equatorial positions around the aluminum atom are preferentially coordinated, depending on the view of rotation. This is in contrast to the polymeric structures 4–7, where the phosphate oxygen atoms occupy axial positions and both nitrogen and oxygen atoms from the ligand occupy equatorial positions. The axial Al–O distance (1.8277 Å) was slightly shorter than the equatorial Al–O distances (1.8507 , 1.8625 , 1.8944 Å). However, the axial Al–N2 distance (2.0380 Å) was almost equal to the equatorial Al1–N1 (2.0356 Å) distance. The Al–O–P bond angles were not equal, with Al1–O3–P1 (164.11°) being greater compared to Al1O4–P1 (160.31°).

3.4. Stability. The most significant aspect of the dealkylation of trialkylphosphate with SAB is the formation of a solid precipitate possessing the covalent Al–O–P linkage. The ease of isolation of the filtered product enhances the potential application as an alkyl phosphate remediation agent. Here, the Al–O bond distances (1.86 – 1.90 Å) are in the range of the literature Al–O covalent bond distances.^{26,28} In addition, the P–O (1.48 – 1.49 Å) bonds involved in bridging of two

adjacent Al centers have a bond length similar to P–O double bond.

A stability study of the Salen aluminum phosphate was carried out. In a typical experiment, compound **4** was suspended in water and the resulting yellow slurry was stirred over a given time. After 3 weeks, the final compound was isolated by filtration and characterized by ^1H and ^{31}P NMR, IR, MS (EI, positive), and melting point. These results all demonstrated the stability of **4** with respect to hydrolysis within the experimental time scale. The ^1H NMR contained peaks corresponding to the ligand and the methoxy groups of the mono-dealkylated phosphate. No peak corresponding to an aldehyde proton was observed. Thus, the imine bonds in the ligand backbone were shown to be stable and still coordinated to the aluminum atom. The ^{31}P NMR had a single peak at δ –6.58, which is upfield compared to trimethylphosphate (δ 3.014) and dimethylphosphate (δ 6.4).²⁹ This suggests that phosphorus is coordinated to the electropositive aluminum center through an Al–O–P bond. Importantly, the presence of only one peak ruled out the release of dealkylated phosphate by hydrolysis of the Al–O bond. These results demonstrate the need for dealkylation technologies that do not readily leach phosphates upon interactions with water. The resulting final product is easy to handle, stable toward quick hydrolysis and leaching, and safe to handle after binding to potentially toxic dealkylated organic phosphates.

4. CONCLUSION

The resulting products from the dealkylation reaction of a series of trialkylphosphates using SAB compounds have been isolated and fully characterized. The isolated products of these reactions are aluminum phosphate compounds where a dealkylated phosphate is covalently bound to an aluminum center through an Al–O–P linkage. These compounds contain six-coordinate aluminum, and the resulting aluminum phosphates are either polymeric or dimeric. This dichotomy in terms of molecular structure, as postulated here, is influenced by the number of methylene units in the salen ligand backbone. However, the bulkiness of the organophosphate alkyl group may also play a role and should be further explored in future research. The phosphates explored in this study could be viable as model compounds for organophosphate chemical warfare agents. Thus, nerve agents can be deactivated and locked into salen units by dealkylation with SAB. Importantly, these aluminum phosphate compounds do not decompose in neutral water, which is an additional advantage to the use of SAB compounds as dealkylation remediation agents. The reaction conditions for all these compounds are very mild. This method could be developed to prepare aluminophosphate ring, cage, or chain structures for soluble models of aluminophosphate materials.

■ ASSOCIATED CONTENT

SI Supporting Information

The Supporting Information is available free of charge at <https://pubs.acs.org/doi/10.1021/acs.inorgchem.0c03244>.

Crystallographic tables, complete crystallographic information file, mass spectra (PDF)

Accession Codes

CCDC 1996252–1996256 contain the supplementary crystallographic data for this paper. These data can be obtained free of charge via www.ccdc.cam.ac.uk/data_request/cif, or by

emailing data_request@ccdc.cam.ac.uk, or by contacting The Cambridge Crystallographic Data Centre, 12 Union Road, Cambridge CB2 1EZ, UK; fax: +44 1223 336033.

■ AUTHOR INFORMATION

Corresponding Author

Rahul R. Butala – Department of Chemistry, University of Kentucky, Lexington, Kentucky 40506-0055, United States; orcid.org/0000-0003-2968-8032; Email: rrbu224@uky.edu

Authors

Sean Parkin – Department of Chemistry, University of Kentucky, Lexington, Kentucky 40506-0055, United States
John H. Walrod – Department of Chemistry, University of Kentucky, Lexington, Kentucky 40506-0055, United States
David A. Atwood – Department of Chemistry, University of Kentucky, Lexington, Kentucky 40506-0055, United States; orcid.org/0000-0002-5284-9714

Complete contact information is available at:

<https://pubs.acs.org/doi/10.1021/acs.inorgchem.0c03244>

Notes

The authors declare no competing financial interest.

■ REFERENCES

- (1) Fields, D. R. Survivors of the Gas Attack in Syria Face Long-Term Illness. *Scientific American* 2017. <https://blogs.scientificamerican.com/guest-blog/survivors-of-the-gas-attack-in-syria-face-long-term-illness/> (accessed 2021-01-02).
- (2) Sellstrom, A.; Cairns, S.; Barbeschi, M. *United Nations Mission to Investigate Allegations of the Use of Chemical Weapons in the Syrian Arab Republic*, Final Report no. A/68/663-S/2013/735; United Nations: New York, 2013.
- (3) Organisation for The Prohibition of Chemical Weapons Fact Sheet 6: *Eliminating Chemical Weapons and Chemical Weapons Production Facilities*, report no. 2017; OPCW, 2017.
- (4) Yang, Y. C. Chemical Detoxification of Nerve Agent VX. *Acc. Chem. Res.* 1999, 32 (2), 109–115.
- (5) Yang, Y. C.; Baker, J. A.; Ward, J. R. Decontamination of chemical warfare agents. *Chem. Rev.* 1992, 92 (8), 1729–1743.
- (6) Florjańczyk, Z.; Wolak, A.; Dębowski, M.; Plichta, A.; Ryszkowska, J.; Zachara, J.; Ostrowski, A.; Zawadzak, E.; Jurczyk-Kowalska, M. Organically Modified Aluminophosphates: Transformation of Boehmite into Nanoparticles and Fibers Containing Aluminodiethylphosphate Tectons. *Chem. Mater.* 2007, 19 (23), 5584–5592.
- (7) Butala, R. R.; Creasy, W. R.; Fry, R. A.; McKee, M. L.; Atwood, D. A. Lewis acid-assisted detection of nerve agents in water. *Chem. Commun.* 2015, 51 (45), 9269–9271.
- (8) Corbridge, D. E. C. *Phosphorus: Chemistry, Biochemistry and Technology*, 6th ed.; CRC Press: Amsterdam, Netherlands, 2013.
- (9) Oliver, S.; Kuperman, A.; Ozin, G. A. A New Model for Aluminophosphate Formation: Transformation of a Linear Chain Aluminophosphate to Chain, Layer, and Framework Structures. *Angew. Chem., Int. Ed.* 1998, 37 (1–2), 46–62.
- (10) Song, Y.; Li, J.; Yu, J.; Wang, K.; Xu, R. Towards Rational Synthesis of Microporous Aluminophosphate AlPO₄–21 by Hydrothermal Combinatorial Approach. *Top. Catal.* 2005, 35 (1–2), 3–8.
- (11) Wang, A.; Xu, R.; Yan, W.; Sun, Y. Synthesis of a New Open-framework Aluminophosphate and the Co-templating Effect in the Crystallization. *Chem. J. Chin. Univ.* 2017, 38 (5), 701–705.
- (12) Wang, M.; Li, J.-y.; Yu, J.-h.; Pan, Q.-h.; Song, X.-w.; Xu, R.-r. Assembly of Helical Hydrogen Bonds in a New Layered Aluminophosphate [C₆N₃H₁₇][Al₂(HPO₄)(PO₄)₂]. *Inorg. Chem.* 2005, 44 (13), 4604–4607.

(13) Medina, M. E.; Iglesias, M.; Gutiérrez-Puebla, E.; Monge, M. A. Solvothermal synthesis and structural relations among three anionic aluminophosphates; catalytic behaviour. *J. Mater. Chem.* **2004**, *14* (5), 845–850.

(14) Chen, P.; Li, J.; Yu, J.; Wang, Y.; Pan, Q.; Xu, R. The synthesis and structure of a chiral 1D aluminophosphate chain compound: d-Co(en)₃[AlP₂O₈]·6.5H₂O. *J. Solid State Chem.* **2005**, *178* (6), 1929–1934.

(15) Lugmair, C. G.; Tilley, T. D.; Rheingold, A. L. Di(tert-butyl)phosphate Complexes of Aluminum: Precursors to Aluminum Phosphate Xerogels and Thin Films. *Chem. Mater.* **1999**, *11* (6), 1615–1620.

(16) Florjańczyk, Z.; Lasota, A.; Wolak, A.; Zachara, J. Organically Modified Aluminum Phosphates: Synthesis and Characterization of Model Compounds Containing Diphenyl Phosphate Ligands. *Chem. Mater.* **2006**, *18* (7), 1995–2003.

(17) Mitra, A.; Atwood, D. A.; Struss, J.; Williams, D. J.; McKinney, B. J.; Creasy, W. R.; McGarvey, D. J.; Durst, H. D.; Fry, R. Group 13 chelates in nerve gas agent and pesticide dealkylation. *New J. Chem.* **2008**, *32* (5), 783–785.

(18) Mitra, A.; DePue, L. J.; Parkin, S.; Atwood, D. A. Five-Coordinate Aluminum Bromides: Synthesis, Structure, Cation Formation, and Cleavage of Phosphate Ester Bonds. *J. Am. Chem. Soc.* **2006**, *128* (4), 1147–1153.

(19) Sheldrick, G. M. A short history of SHELX. *Acta Crystallogr., Sect. A: Found. Crystallogr.* **2008**, *64*, 112–122.

(20) Sheldrick, G. M. SHELXT - Integrated space-group and crystal-structure determination. *Acta Crystallogr., Sect. A: Found. Adv.* **2015**, *71*, 3–8.

(21) Sheldrick, G. M. Crystal structure refinement with SHELXL. *Acta Crystallogr., Sect. C: Struct. Chem.* **2015**, *71*, 3–8.

(22) Keizer, T. S.; De Pue, L. J.; Parkin, S.; Atwood, D. A. Catalytic Dealkylation of Phosphates with Binuclear Boron Compounds. *J. Am. Chem. Soc.* **2002**, *124* (9), 1864–1865.

(23) Lee, J. D. *Concise Inorganic Chemistry*, 5th ed.; Wiley-Blackwell: New York, 1999.

(24) Munoz-Hernandez, M.-A.; Keizer, T. S.; Wei, P.; Parkin, S.; Atwood, D. A. Reactivity and Derivatization of Five-Coordinate, Chelated Aluminum. *Inorg. Chem.* **2001**, *40* (26), 6782–6787.

(25) Wang, Y.; Parkin, S.; Atwood, D. Six-coordinate aluminium phosphinate. *Chem. Commun.* **2000**, *18*, 1799–1800.

(26) Wang, Y.; Parkin, S.; Atwood, D. Ligand–Tetrahydrofuran Coupling in Chelated Aluminum Phosphinates. *Inorg. Chem.* **2002**, *41* (3), 558–565.

(27) Pinkas, J.; Chakraborty, D.; Yang, Y.; Murugavel, R.; Noltemeyer, M.; Roesky, H. W. Reactions of Trialkyl Phosphates with Trialkyls of Aluminum and Gallium: New Route to Aluminogallophosphate Compounds via Dealkylsilylation†. *Organometallics* **1999**, *18* (4), 523–528.

(28) Richeter, S.; Thion, J.; van der Lee, A.; Leclercq, D. Synthesis, Structural Characterization, and Properties of Aluminum (III) meso-Tetraphenylporphyrin Complexes Axially Bonded to Phosphinate Anions. *Inorg. Chem.* **2006**, *45* (25), 10049–10051.

(29) Ghanem, E.; Li, Y.; Xu, C.; Raushel, F. M. Characterization of a Phosphodiesterase Capable of Hydrolyzing EA 2192, the Most Toxic Degradation Product of the Nerve Agent VX†. *Biochemistry* **2007**, *46* (31), 9032–9040.